Power scaling of femtosecond enhancement cavities and high-power applications

Ioachim Pupeza[a,b], Tino Eidam[c], Jan Kaster[a,b], Birgitta Bernhardt[a], Jens Rauschenberger[a,b], Akira Ozawa[a], Ernst Fill[a], Thomas Udem[a], Matthias F. Kling[a], Jens Limpert[c], Zeyad A. Alahmed[d], Abdallah M. Azzeer[d], Andreas Tünnermann[c], Theodor W. Hänsch[a,b], Ferenc Krausz[a,b]

[a]Max-Planck-Institut für Quantenoptik,
Hans-Kopfermann-Strasse 1, 85748 Garching, Germany;
[b]Ludwig-Maximilians-Universität München, Department für Physik,
Am Coulombwall 1, 85748 Garching, Germany;
[c] Friedrich-Schiller-Universität Jena, Institut für Angewandte Physik,
Albert-Einstein-Strasse 15, 07745 Jena, Germany;
[d] King Saud University, Department of Physics and Astronomy,
P.O. Box 2455, 11451 Riyadh, Saudi Arabia

ABSTRACT

An Yb-based 78-MHz repetition rate fiber-amplified frequency comb is used to investigate the power scaling limitations of a standard-design bow tie high-finesse enhancement cavity for XUV generation. With a Xenon gas jet in the 22-μm-radius focus, the 200-fs intra-cavity circulating pulse reaches a maximum of 20 kW of time-averaged power. A novel cavity design is presented, conceived to overcome the observed enhancement limitations and offering the prospect of few-nm high-power high-harmonic generation. Several applications which come into reach for the first time are discussed.

Keywords: Enhancement cavity, XUV, MHz high-harmonic generation

1. INTRODUCTION

Short-wavelength radiation in the VUV and XUV regions has a number of exciting applications, summarized in Refs. 1,2. It can be used in XUV microscopy and tomography,[3] interferometry and holography,[4] plasma physics,[5] spectroscopy,[6] at-wavelength-testing of components for EUV lithography[7] and surface and material studies,[8] just to name the most prominent ones. Some of these applications have only been demonstrated using synchrotron radiation. The availability of a table-top source of bright VUV and XUV radiation would undoubtedly result in a significant boost of pertinent experiments. Over the past few decades, the development of high-power ultrafast lasers motivated intense research in the field of high-harmonic generation (HHG) as a table-top source of XUV radiation. One of the most prominent state-of-the-art HHG techniques relies on the enhancement of high-repetition-rate laser pulses inside of a high-finesse passive resonator, also called "enhancement cavity".[9–14] Due to the lack of components prone to high intensities, a passive resonator offers an increased robustness compared to active laser cavities. In an intra-cavity focus, peak intensities exceeding 10^{13} W/cm^2 can be reached at MHz repetition rates. On the one hand, these intensities are necessary to trigger the highly nonlinear processes in a noble gas target, customarily employed for HHG. On the other hand, the overall conversion efficiency of the fundamental radiation to the XUV can be increased by the enhancement in the passive cavity. Furthermore, many applications might benefit from the high repetition rates of intra-cavity HHG.

The enhancement in a passive resonator is based on the interferometrical overlap of the seeding laser electric field with the field circulating inside the cavity. In this manner, energy from the seeding laser is continuously

Further author information: (Send correspondence to Ioachim Pupeza)
E-mail: ioachim.pupeza@mpq.mpg.de, Telephone: +49 (0)89 289 14637

Fiber Lasers VIII: Technology, Systems, and Applications, edited by Jay W. Dawson, Eric C. Honea,
Proc. of SPIE Vol. 7914, 79141I · © 2011 SPIE · CCC code: 0277-786X/11/$18 · doi: 10.1117/12.877532

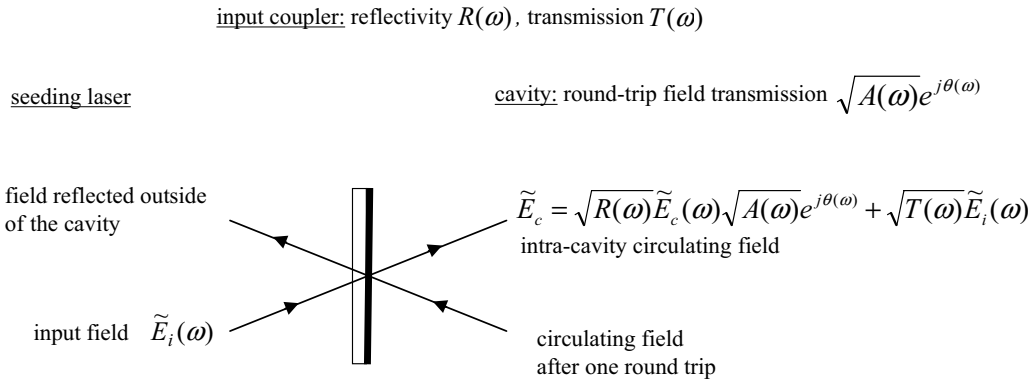

Figure 1. Electric fields at the input coupler of an enhancement cavity in the steady state.

coupled to the cavity. The enhancement-limiting effects can be divided into two categories. Firstly, intra-cavity losses attenuate the electric field amplitude upon each round trip. Secondly, in the case of significantly large optical bandwidths, intra-cavity dispersion affects the circulating electric field, leading to a suboptimal overlap with the seeding field and, thus, to a limitation of the enhanced spectrum. In the high-power case, where nonlinear effects related to the intra-cavity propagation of the fundamental beam can not be neglected anymore, both enhancement-limiting mechanisms exhibit intensity-dependent behavior. The enhancement cavities built to this day can be classified in three categories, defined by their seeding laser sources. Due to the specific intensity and bandwidth regime of these sources, each category exhibits characteristic enhancement-limiting effects. Firstly, continuous-wave passive cavities with enhancement factors on the order of 10^5 have been demonstrated in the early nineties, see e.g. Ref. 15. Such cavities were e.g. used to enhance the measurement sensitivity of optical losses. Secondly, with the advent of Ti:Sa-based frequency combs, ultrashort pulses were enhanced for the first time for HHG at repetition rates of several tens of MHz.[9,10] Due to their broad optical bandwidth, Ti:Sa lasers enable high peak intensities through the short pulse duration rather than the average power. The shortest intra-cavity pulse duration of 27 fs has been achieved with a power enhancement of 50 by seeding a broadband cavity with 20 fs pulses.[9] Thirdly, Yb-based frequency combs were employed for intra-cavity HHG due to their significantly larger average power compared to Ti:Sa systems.[13,16] So far, the largest circulating powers in an ultrafast enhancement cavity lie in the multi-10-kW range and have been demonstrated with our Yb-based system.[14] For some applications, the only drawback of Yb-based seeding lasers as compared to Ti:Sa systems is the relatively narrow available optical bandwidth. However, nonlinear pulse compression of the seeding pulses offers the prospect of the enhancement of few-10-fs Yb-based pulses.

In our group, two aims are currently pursued with Yb-based enhancement cavities: the enhancement of nonlinearly compressed few-10-fs pulses in a high-finesse resonator and the enhancement of few-100-fs pulses to MW-level circulating average powers. This paper reviews our recent progress towards these aims and gives an outlook on some of the applications that come into reach once these aims will be achieved. In Section 2 we introduce our experimental setup and discuss the recent power scaling investigations. Section 3 addresses current developments en route to our two aims. In Section 4 prospective applications are presented and Section 5 concludes the paper.

2. HIGH-POWER RESONANT CAVITY ENHACEMENT

2.1 Theoretical Background

The structure of an enhancement cavity setup consists of three main components: a seeding laser, a passive resonator and a synchronization scheme between those. In the following, we give a brief introduction to these three components with an emphasis on laser-cavity synchronization aspects.

Figure 1 shows the complex electric fields at the input coupler (IC) of an enhancement cavity in the steady state. In the following derivation we assume perfect transverse mode matching at the IC, i.e. that the seeding laser

beam is matched to the excited cavity transverse mode. For each frequency component ω, the single-round-trip power attenuation and accumulated phase are denoted by $A(\omega)$ and $\theta(\omega)$, respectively. One cavity round trip of the circulating electric component $\widetilde{E_c}(\omega)$ can be completely described by its multiplication by $\sqrt{A(\omega)}\exp[j\theta(\omega)]$. Let $R(\omega)$ denote the IC power reflectivity, such that a reflection at the IC implies the multiplication of the impinging electric field by $\sqrt{R(\omega)}$. Let $T(\omega)$ denote the IC power transmission. Resonant enhancement requires the constructive interference of the intracavity field reflected by the IC, i.e., $\sqrt{R(\omega)}\ \widetilde{E_c}(\omega)\ \sqrt{A(\omega)}\exp[j\theta(\omega)]$ with the portion of the input field transmitted through the IC, i.e., $\sqrt{T(\omega)}\ \widetilde{E_i}(\omega)$. In the steady state, the sum of these two interfering fields equals $\widetilde{E_c}(\omega)$:

$$\widetilde{E_c}(\omega) = \sqrt{R(\omega)}\ \widetilde{E_c}(\omega)\ \sqrt{A(\omega)}\exp[j\theta(\omega)] + \sqrt{T(\omega)}\ \widetilde{E_i}(\omega) \tag{1}$$

$$\Leftrightarrow \widetilde{H}(\omega) := \frac{\widetilde{E_c}(\omega)}{\widetilde{E_i}(\omega)} = \frac{\sqrt{T(\omega)}}{1-\sqrt{R(\omega)A(\omega)}\exp[j\theta(\omega)]}. \tag{2}$$

Equation (2) reveals that frequency-dependencies of $\sqrt{A(\omega)}$ and $\exp[j\theta(\omega)]$ affect both the amplitude and the phase of $\widetilde{H}(\omega)$ and, thus, of the circulating field. Several methods for the measurement of these quantities have been developed. The technique presented in Ref. 17 enables for the first time a highly sensitive measurement of these quantities in a cavity including nonlinear effects.

Due to the comb-like structure of the frequency-resolved response function $\widetilde{H}(\omega)$, a very efficient way of cavity enhancement is its illumination with a single frequency or a frequency comb. The modes of a frequency comb producing ultrafast pulses can be assumed to be equidistant:

$$\omega_N = N\omega_r + \omega_{CE}. \tag{3}$$

Here, N is the comb mode number, ω_r the laser repetition frequency and ω_{CE} is the carrier-envelope offset frequency[18] (all frequencies are angular frequencies). For an optimum enhancement, the seeding frequency comb modes and the cavity resonances need to overlap in the frequency domain at all times. This situation is sketched in panel (a) of Figure 2. On the one hand, the absence of intra-cavity higher-order dispersion, i.e. a close-to-linear frequency dependence of $\theta(\omega)$, over the enhanced spectrum is required. This must be provided by the cavity optics. On the other hand, the relative frequency jitter between the seeding laser comb modes and the cavity resonances needs to be removed. Usually, the enhancement in high-finesse cavities requires active control of at least one degree of freedom. The necessity of actively controlling a second degree of freedom mainly depends on the jitter, on the cavity finesse and on the stability of the enhanced frequency comb. For many practical applications, fluctuations of two orthogonal degrees of freedom, e.g. of ω_r and ω_{CE} around the state of optimum overlap have a very similar effect on the enhancement. In these cases, usually the control of the repetition frequency is chosen, since it is the most straight-forward comb control from the experimental point of view. In the following, we investigate quantitatively under which conditions this single control is sufficient.

For our derivation, we assume that the central optical frequency ω_C is being locked to the peak of a corresponding cavity resonance by actively controlling solely the repetition frequency ω_r of the comb and we calculate the effect of a variation $\Delta\omega_{CE}$ of the other comb parameter ω_{CE} on the enhancement. For simplicity, here we assume a dispersion-free cavity and an initial ω_{CE}, which leads to an optimum overlap of the seeding comb modes with the cavity resonances, see Figure 2.a. Let N_C denote the mode number of ω_C, such that

$$\omega_C = N_C\omega_r + \omega_{CE} \tag{4}$$

holds. A variation of the comb parameter ω_r, meaning a change of the comb mode spacing, can be entirely compensated by the active control. In contrast, a variation $\Delta\omega_{CE}$ of the carrier-envelope offset frequency shifts the entire frequency comb, as depicted in Figure 2.b. The active control compensates the drift of ω_C by introducing a variation $\Delta\omega_r$ to ω_r:

$$\omega_C = N_C(\omega_r - \Delta\omega_r) + \omega_{CE} + \Delta\omega_{CE}. \tag{5}$$

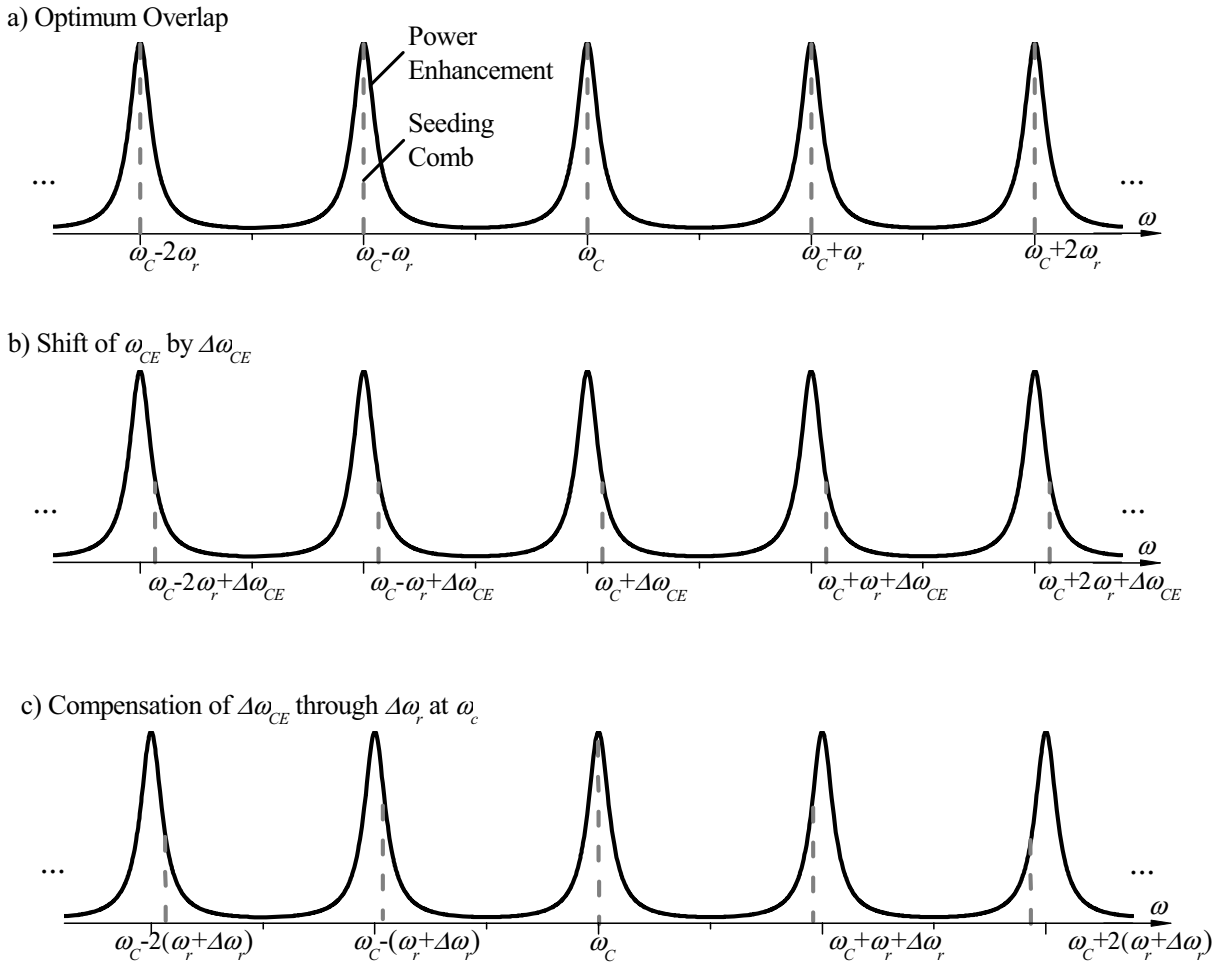

Figure 2. Illustration of the effect of a shift $\Delta\omega_{CE}$ of the carrier-envelope offset frequency ω_{CE} on the enhanced frequency comb, if the laser-cavity lock is realized by controlling the repetition frequency ω_r such that the central optical frequency ω_C is locked to the peak of a cavity resonance.

The last two equations imply:

$$\Delta\omega_r = \Delta\omega_{CE}/N_C. \tag{6}$$

While the mode with the number N_C retains its initial frequency, the mode with the number $N_C + m$ will experience a frequency shift equal to $m\Delta\omega_r$. This situation is depicted in Figure 2.c.

In Figure 3, the effect of a variation $\Delta\omega_{CE}$, corrected by a variation of ω_r as described above, on the intra-cavity spectrum is plotted for several enhancement factors and several optical bandwidths (Gaussian input spectra are assumed). As a result of this correction, the circulating power decreases and the intra-cavity spectrum is narrowed relative to the case of optimum overlap of the seeding comb with the cavity resonances. The two relative changes are plotted as functions of $\Delta\omega_{CE}$ and of $\Delta\omega_{CE}$ related to the full-width-half-maximum of the cavity resonance ($FWHM_{Resonance}$). The optical bandwidths used in the calculated examples represent typical values for Yb systems.

2.2 Experimental Setup

Figure 4 depicts the experimental setup. The seeding laser system (see Figure 4.a) is described in detail in Ref. 19. The pulses are generated by a passively mode-locked, diode-pumped Yb:KYW oscillator and are amplified in

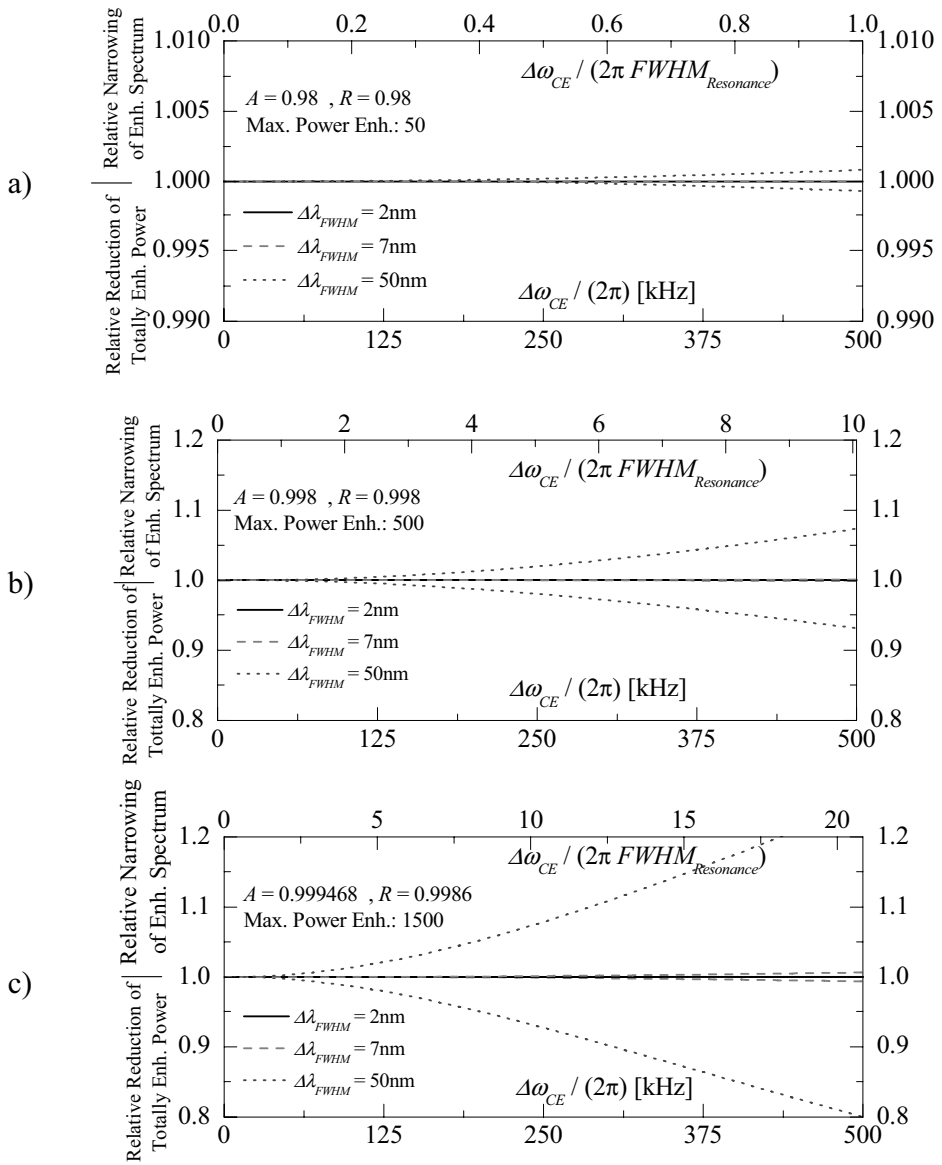

Figure 3. Reduction of the totally enhanced power (i.e. integrated over the spectrum) and spectral narrowing of the intra-cavity circulating pulse after a carrier-envelope offset frequency drift $\Delta\omega_{CE}$ has been compensated by a shift of the repetition frequency ω_r, locked at the central optical frequency ω_C. Both values are related to the case of optimum overlap between the frequency comb modes and the cavity resonances. The upper abscissa is related to the full-width-half-maximum of the cavity resonance $FWHM_{Resonance}$. Gaussian input spectra are assumed. a) and b): power enhancement at ω_C of 50 and 500, respectively and impedance matching, i.e. the input coupler reflectivity R equals the cavity round-trip transmission A. c) power enhancement at ω_C of 1500. This case corresponds to our experimental setup.

a two-stage fiber-based chirped pulse amplifier system. The stretcher and compressor are implemented with transmission gratings. At the output of the main amplifier, the 78 MHz repetition rate pulse train reaches up to 50 W of average power. The central wavelength is 1042 nm. By varying the distance between the two compressor gratings, the pulse duration can be adjusted between 200 fs, corresponding to almost bandwidth-limited pulses, and more than 10 ps with a negligible effect on other beam parameters. The pulses can be compressed down to 27 fs in a subsequent nonlinear compression stage consisting of a short piece of photonic-crystal fiber followed by several bounces on a pair of chirped mirrors.[19] However, in all experiments mentioned in this work, this stage

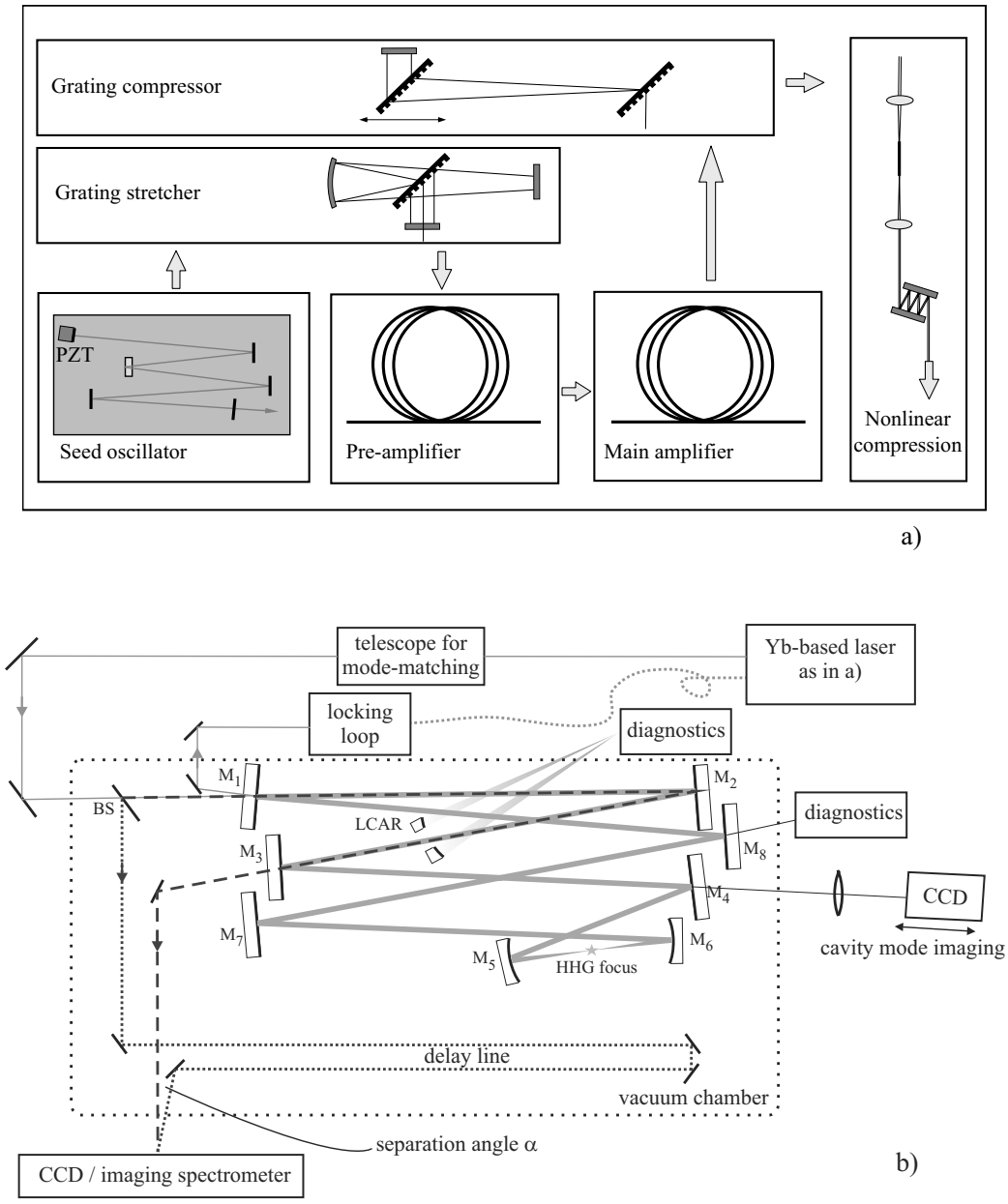

Figure 4. Experimental setup: a) seeding laser[19] and b) enhancement cavity. M2-M8: dielectric mirrors with R=99.995%±20ppm (ring-down measurement), M1: 99.86%-reflectivity input coupler. M5 and M6 have a radius of curvature of 150 mm and enclose the 22 μm cavity focus ($1/e^2$-radius calculated at the stability range center). LCAR: large circular aperture reflector, diagnostics: photodiode / power meter / spectrometer / autocorrelator / beam profiler. Dotted and dashed lines: two arms of an interferometer, overlapping a (delayed) copy of the input pulse with a copy of the circulating input pulse on a CCD camera or an (imaging) sprectrometer.

has been bypassed for seeding the enhancement cavity. Details on the nonlinear compression are discussed in Section 3.3.

As in the work presented in Refs. 9–13, our enhancement cavity is a standard-design bow tie ring resonator whose round-trip time is adjusted to the inverse of the seeding laser repetition rate (see Figure 4.b). For compactness, the beam is folded several times. The $1/e^2$ beam diameters on the cavity mirrors range between

1.5 and 2.6 mm. To minimize the cavity group-delay dispersion (GDD) and losses it is placed inside a vacuum chamber. Its optics (Layertec) exhibit very low dispersion (GDD < 20 fs^2 per mirror, according to manufacturer specification) over a bandwidth of more than 100 nm around the central optical wavelength of the seeding laser, making further dispersion compensation unnecessary.

A stable lock of the seeding laser to the enhancement cavity is achieved by actively controlling a single comb parameter. In our case, this control is obtained by varying the position of an oscillator cavity end mirror with a fast piezoelectric transducer (PZT). The error signal for the lock is generated with a Hänsch-Couillaud scheme[20] for a narrow wavelength range which is selected with a grating and a slit. In our case, the necessary polarization discrimination is caused by the polarization-dependent cavity losses owed to the non-orthogonal incidence on the mirrors, in contrast to the original scheme[20] where an intra-cavity Brewster plate is employed. In addition, for optimum enhancement a coarse CE-offset adjustment is achieved by manually varying the seed oscillator optical pump power. The FWHM bandwidth of the 200 fs pulses corresponds to roughly 7 nm. Typical power enhancement factors range between 1400 and 1800 (see Ref. 14). The effect of ω_{CE}-variations on the lock can be estimated according to Figure 3.c. This calculation shows that ω_{CE}-variations even on the order of several times the cavity resonance FWHM can be compensated by our locking scheme with a minor effect on the circulating pulse energy and spectrum.

We determine the circulating average power by two different methods. Firstly, we measure the power leaking through a highly reflective cavity mirror and divide it by the mirror transmission, which was measured beforehand and amounts to 1.65 ppm. In order to prevent measurement errors due to potential mirror transmission changes at higher powers, we implement a second circulating power measurement method using a large circular aperture around the cavity beam (see Figure 4.b). This aperture does not affect the enhancement but still reflects a measurable portion of the intra-cavity light. A possible power / intensity-dependence of the diagnostic mirror transmission results in a deviation of the ratio of the values measured with the two methods. Moreover, by using the leakage through the diagnostic mirror we monitor the cavity transverse mode with a CCD camera and measure the intra-cavity autocorrelation and spectrum.

An important diagnostic for the intra-cavity circulating light is the measurement of the phase difference between the circulating and the seeding electric fields by means of (spatial-)spectral interferometry. This method was first described in Ref. 17 and combines the phase sensitivity of a high-finesse resonant cavity with the power and intensity enhancement achieved therein. Modifications of the single-round-trip GDD on the order of less than 1 fs^2, which can e.g. be caused by intra-cavity nonlinear effects, are measurable.

2.3 Enhancement Limitations

In Ref. 14, the circulating time-averaged power and pulse peak power scalability of our cavity was investigated. Throughout these experiments, the fundamental Gaussian transverse mode of the cavity was excited. The circulating power level, up to which the cavity response can be considered linear, is roughly 20 kW for a constant intra-cavity pulse duration of 200 fs. Beyond this power level, resonator instabilities occur, which can be removed by chirping the seeding laser pulses by means of varying the distance between the compressor gratings. With a constant seeding power of 50 W and pulse durations of 2 ps and more, a maximum intra-cavity average power of 72 kW was obtained. Compressing the pulses below 2 ps with the same seeding power caused a power enhancement decrease, leading to the conclusion that intensity-related effects are the primary cause of enhancement limitations, rather than only time-averaged circulating power. This conclusion is confirmed by results in Ref. 17. The cavity was shown to have a constant round trip GDD of around -5 fs^2 for circulating pulse peak powers of up to 400 MW. When the peak power was increased beyond this value, either by means of increasing the seeding average power or by reducing the pulse duration, a significant increase of the round trip GDD magnitude can be observed (up to -14 fs^2 for 900 MW of peak power).

Moreover, in Ref. 14 an average-power dependent radius variation of the cavity mode is reported. Since the cavity eigenmode, which we excited in these experiments is defined by the cavity optics and the optical properties of the intra-cavity propagation path, this observation indicates thermal effects in the latter two. Operating the cavity in intensity regimes beyond the threshold values discussed above, results reproducibly in mirror damage. Figure 5 shows the magnified images of typical cavity mirror damages. The physical mechanism of the damages is subject to further investigation.

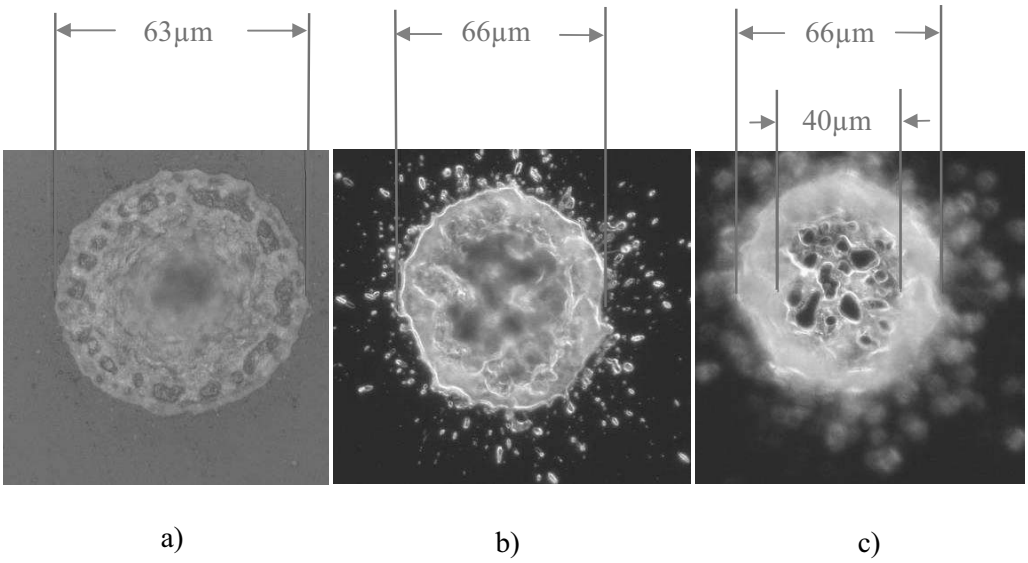

Figure 5. Optical microscope images of enhancement cavity mirror damages: a) input coupler, b) and c) same cavity high reflector, two different focusing depths of the optical microscope.

There are two independent approaches of circumventing the intensity-related limitations. The first approach increases the laser spot size on the mirrors thus decreasing the incident intensity and mirror-related nonlinear effects. Moreover, a larger irradiated area decreases the thermal gradient, which is beneficial for the high-average-power regime. Secondly, for a given cavity design, the threshold up to which the cavity behaves linearly with respect to the input field could be increased by means of mirror development. In this work we address the first approach. In Section 3.2 we report on an enhancement cavity design with enlarged laser spot sizes on the mirrors.

2.4 Inclusion of an Intra-Cavity Gas Target

We were able to achieve the upper circulating power limit of 20 kW for an intra-cavity pulse duration of 200 fs, including a Xenon jet in the cavity focus. As nozzle we used a tapered glass tube, with an opening of approximately 80 μm. The backing pressure was 3 bar. In order to achieve the shortest circulating pulse duration, a slight pre-chirp of the input pulses was necessary. This can be understood by expressing the circulating field $\widetilde{E_c}(\omega)$ from Equation (2) as:

$$\widetilde{E_c}(\omega) = \widetilde{E_i}(\omega)\frac{\sqrt{T(\omega)}}{1-\sqrt{R(\omega)A(\omega)}\exp[j\theta(\omega)]}. \tag{7}$$

In order to obtain a short circulating pulse, the phase of $\widetilde{E_c}(\omega)$ needs to be as flat as possible. While the (nonlinear) cavity round-trip dispersion contained in θ affects the phase of right-hand side of the above equation, the same phase can be "flattened" using the phase of the input field $\widetilde{E_i}(\omega)$, i.e. by applying a pre-chirp to the seeding pulses. The characterization of the generated XUV light is subject to current study.

3. CURRENT DEVELOPMENTS

3.1 XUV Output Coupling

Several applications (see Section 4) require the output coupling of the XUV light generated in the gas target from the cavity. Due to the collinear propagation of the high harmonics and the fundamental radiation generating them, one of the most challenging aspects of intra-cavity HHG remains coupling out the XUV light without severely affecting the fundamental radiation. Currently, the circulating power inside a HHG enhancement cavity including an output coupler is limited by the latter and, to the best of our knowledge, amounts to a few kW, meaning a significantly lower level than demonstrated in a cavity without an output coupler.[14] The output

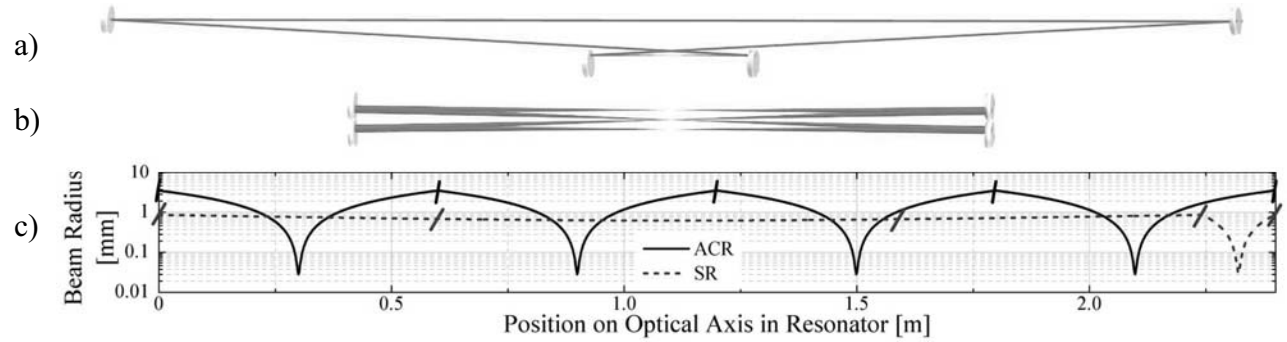

Figure 6. Comparison between a standard design resonator (a) and an all-curved-mirror resonator (b). Part (c): beam radii on the resonator mirrors. The transversal lines indicate the mirror positions along the optical axis, their inclination corresponds to the angles of incidence.

couplers of the first demonstrated HHG enhancement cavities were thin plates, placed at Brewster's angle in the fundamental beam after the HHG focus.[9,10,12] The generated XUV light, for which the refractive index of the plate material is lower than 1, experiences total reflection and is coupled out of the cavity. So far, the largest circulating average power we achieved with an intra-cavity Brewster plate was 5 kW for a 0.2 mm thick SiO_2 plate and a 200 fs circulating pulse duration. Thermal and / or nonlinear effects in the plate led to a coupling among transverse cavity higher-order modes,[21] which could be suppressed by choosing a proper position within the stability range and by using spatial filters. The major drawback of this output coupling technique consists in thermal and nonlinear effects, which constitute a fundamental power scaling limitation.

Alternative approaches include a nanostructure, written in the last layer of the cavity mirror following the HHG focus[13] acting as a highly reflecting mirror for the fundamental radiation and as a diffraction grating for the XUV, thus providing the necessary spatial separation. However, so far the circulating power achieved with such an output coupler is also limited to 5 kW.[16] Recent results in Ref. 22 show enhanced third harmonic generation at the surface of such an element. This suggests that intensity-dependent local field enhancement effects are not negligible in the intensity regime of a high-power enhancement cavity. Moreover, the spatial dispersion of different harmonics might be a disadvantage for several applications.

Currently, we investigate the possibility of collinearly output coupling the XUV through an on-axis aperture in the mirror following the HHG focus as the most promising approach from the point of view of power and intensity scalability. For comparison we employ either the fundamental transverse mode of the cavity or a field distribution that avoids the aperture. The novel technique of quasi-imaging allows the latter without a significant decrease of the cavity finesse.[23]

3.2 Large-Spot-Size Resonator Design

An approach to significantly pushing the identified intensity-related enhancement limitations consists in increasing the spot sizes on the cavity mirrors. This can be achieved by operating an all-curved-mirror resonator (ACR) close to the border of its stability range. In Figure 6, a standard-design resonator (SR) in the stability range center, similar to the ones employed in Refs.[9–14,17] is compared to an ACR, consisting of 4 mirrors with equal radii of curvature (300 mm). For comparison reasons, the repetition rate of both resonator designs was set to 250 MHz (with two pulses circulating in the cavity) and the focus radius to 30 μm. Figure 6.c shows the spot sizes on the mirrors. In the ACR, the spot area is increased by more than 14 times with respect to the SR, suggesting that at the same intensity on the mirrors an average power higher by more than an order of magnitude can be achieved. In conjunction with a modified version of the CPA system described in Ref.,[24] which is planned to seed our ACR, circulating average powers in the Megawatt range for ultrashort MHz-repetition-rate pulses come into reach for the first time. On the other hand, the ACR offers the prospect of enhancing pulses of reduced duration by nonlinear compression of the seeding pulses, as discussed in the next section.

3.3 Enhancement of Nonlinearly Compressed Pulses

The nonlinear compression stage shown in Figure 4.a, consists of a short piece of fiber and a pair of chirped mirrors. In a first step the signal is coupled into the microstructured effectively single-mode fiber and spectrally broadened therein. The fiber has a length of about 6 cm and a mode field diameter of 35 μm. Typically, a coupling efficiency to the fundamental mode of more than 90% can be achieved. Because of the short nonlinear interaction length it is possible to remove the imposed chirp with a pair of chirped mirrors instead of using a pair of prisms. These mirrors are designed to exhibit a group velocity dispersion of -250 fs^2 in a spectral range from 1000 nm to 1080 nm for perpendicular incidence. The advantages are a simple alignment and a compact, polarization-independent setup. At the output of this stage, pulses with 27 fs duration and a peak power of 20 MW at 57 W of average power could be achieved.[19]

Enhancing the spectrally broadened pulses in a passive cavity exhibits three major challenges. Firstly, the effect of the cavity single-round-trip dispersion on the circulating pulse in the steady state is magnified by a factor on the order of the power enhancement.[17] Thus, special mirror designs with low GDD and / or the use of pairs of mirrors with opposite GDD are necessary. Research on an optimum mirror design is currently being performed in our group. Secondly, amplitude and phase fluctuations stemming from the nonlinear spectral broadening process might hamper the resonant enhancement. To the best of our knowledge, spectrally broadened pulses have not yet been enhanced in a passive resonant cavity. And finally, as suggested by the 50 nm cases in Figure 3, locking the seeding laser comb to the cavity might require the active control of an additional degree of freedom.

4. OUTLOOK ON APPLICATIONS

4.1 Coincidence Spectroscopy of Correlated Electron Dynamics

Of particular interest in atomic and molecular physics is to gain a more detailed understanding of the role of electron correlation in the unfolding dynamics when an atom or molecule is excited by an ultrashort light pulse. Examples for processes, where electron correlation play a role, are the creation of doubly excited states[25] and the (non-sequential) double ionization of atoms and molecules[26,27] with excitation energies in the XUV region. In order to explore correlated electron dynamics in detail, momentum imaging techniques are necessary, with the particular advantage of coincident detection of multiple charged particles such as for the reaction microscope (REMI, see e.g. Ref. 28). Using this technique, for each laser-induced ionization event, both the generated ions and electrons can be detected simultaneously with high efficiency. The coincident detection of charged particles, however, requires keeping the ionization rate and target density low, such that there is typically less or even much less than a single event per laser shot. In addition, the more ions or electrons need to be recorded in coincidence, the less likely their coincident detection is. Therefore, in order to achieve high-quality statistical data, high-repetition rate laser sources are required. Enhancement cavities operating at MHz repetition rates provide at least two opportunities to achieve a major step forward in the understanding of correlated electron dynamics when combined with REMI detection: (i) circulating infrared fields with extremely high peak power, leading to intensities in the focus of the cavity on the order of up to 10^{14} - 10^{15} W/cm^2, which can be used to introduce (non-sequential) double ionization, and (ii) XUV light pulses in the relevant energy range for reaching e.g. doubly-excited states can be generated in the focus of the cavity (and coupled out for their use in external experiments). In the first application the enhancement cavity setup would incorporate a thin gas jet and a REMI. In the second application, the REMI can be external to the cavity. With some further development, pump-probe experiments using both the intense infrared as well as XUV pulses inside an enhancement cavity may be feasible. The described applications of MHz enhancement cavities have promising potential for studying the complex physics of correlated processes in much more detail.

4.2 Photoelectron Emission Microscopy (PEEM) Studies of Electron Dynamics in Nanostructures

The dynamics of electrons and fields on the nanoscale are of interest to a wide spectrum of scientists, ranging from physicists, chemists and materials scientists to biologists. Recent advances allow metal surfaces to be structured and characterized on the nanometer scale. They allow us to localize light fields on the same scale, which in turn enables us to control the properties of nanolocalized fields to reveal new aspects of their underlying

science and to tailor them for specific applications. When few-cycle laser pulses illuminate a metal nanostructure, ultrafast nanoplasmonic field dynamics unfolding on timescales down to the attosecond regime can be initiated. Until now, the attosecond dynamics of nanoplasmonic fields have not been directly observed with simultaneous attosecond temporal and nanometer spatial resolution. Hence an experimental study of those ultrafast and nanolocalized plasmonic field dynamics is of particular importance and requires an instrument which combines both ultrahigh spatial and ultrahigh temporal resolution. As a suitable approach, Stockman et al. suggested to combine photoelectron emission microscopy (PEEM) with attosecond metrology: first a few-cycle light pulse excites collective electron dynamics which is then temporally and spatially imaged by photoelectrons released by a time-delayed attosecond XUV probe pulse.[29] In a first attempt to combine PEEM with kHz repetition rate XUV sources, space charge was found to severely limit the applicable XUV energy per pulse,[30] resulting in acquisition times, which are realistically too long for an attosecond time-resolved experiment in conjunction with few-kHz XUV sources. It is thus highly desirable to implement attosecond PEEM measurements of nanoplasmonic fields with a high-repetition rate XUV source. The necessary light pulses for the experiment could be derived using an enhancement cavity: the pump pulse for the (resonant) excitation of the nanostructures in the infrared can be split off before the cavity. As only low pulse energy is needed for the excitation, this will still leave enough energy to create the XUV probe pulses within the enhancement cavity. The XUV will be coupled out from the cavity to be temporally and spatially overlapped with the excitation pulse on the nanosample. This approach might allow the realization of attosecond PEEM studies for the first time.

4.3 Relativistic Thomson Scattering as a Source of Hard X-Rays

An alternative way for converting the laser light to short wavelength radiation involves scattering the laser pulse from a relativistic electron pulse.[31] The relativistic Doppler shift leads to an increase of the photon energy by a factor $4\gamma^2$, where γ is the relativistic mass factor of the electrons. A 50 MeV electron beam thus generates 50 keV X-rays from 1.2 eV photons. Due to the small Thomson cross-section, a high laser pulse energy and high charge of the electron bunch are required for generating a useful number of X-ray photons. However, the weak nature of the interaction may be considered an advantage in case of an enhancement cavity since it induces negligible depletion of the circulating laser pulses.[32]

We point out that the cavity design shown in Figure 6.b is particularly suitable for Thomson scattering applications. Its geometry allows straightforward insertion of the electron pulse and extraction of the X-rays generated. If the electrons collide at a small angle with the laser pulse, only a small downshift of the X-ray photon energy is induced.

4.4 Other Applications of Enhancement Cavities

The high circulating power in the cavity combined with the high repetition rate affords applications of enhancement cavities in quite different fields of research. We mention multiphoton entanglement experiments,[33] cavity-enhanced scattering,[34] ultrasensitive absorption and dispersion spectroscopy,[35] precision spectroscopy with helium[36] and the generation of quantum frequency combs.[37] For a successful realization of these applications a high circulating power is of crucial importance.

5. CONCLUSION

We have investigated the power scaling limitations of a 78-MHz repetition rate standard-design bow-tie high-finesse enhancement cavity for XUV generation, seeded by an Yb-based CPA frequency comb. With a Xenon gas jet in the 22-μm-radius focus, a maximum of 20 kW of time-averaged intra-cavity power was achieved with a circulating pulse duration of 200 fs. A stable laser-cavity lock was realized with the active control of a single frequency comb parameter.

A novel cavity design is presented, conceived to overcome the observed enhancement limitations and to push these to the Megawatt circulating power range in conjunction with a state-of-the-art seeding source. Furthermore, the option of spectrally broadening the seeding pulses and, thus, compressing them in the time domain is discussed. With these advances, several applications like coincidence spectroscopy of correlated electron dynamics, photoelectron emission microscopy studies of electron dynamics in nanostructures and relativistic Thomson scattering come into reach for the first time as MHz-repetition-rate table-top experiments.

ACKNOWLEDGEMENTS

This work was supported by the Deutsche Forschungsgemeinschaft (DFG) via SPP1391 and the Cluster of Excellence, Munich Centre for Advanced Photonics (MAP) (www.munichphotonics.de), by the KORONA Max-Planck-Institut für Quantenoptik (MPQ)/Fraunhofer Institut für Lasertechnik (ILT) cooperation, by the BMBF via PhoNa (Photonische Nanomaterialien). The authors gratefully acknowledge the support of the Helmholtz-Institut Jena.

REFERENCES

[1] Attwood, D., [*Soft X-rays and Extreme Ultraviolet Radiation*], Cambridge University Press, Cambridge (1999).

[2] Jaegle, P., [*Coherent Sources of XUV Radiation*], Springer, New York (2006).

[3] Barty, A., Boutet, S., Bogan, M., Hau-Riege, S., Marchesini, S., Sokolowski-Tinten, K., Stojanovic, N., Tobey, R., Ehrke, H., Cavalleri, A., Düsterer, S., Frank, M., Bajt, S., Woods, B. W., Seibert, M. M., Hajdu, J., Treusch, R., and Chapman, H. N., "Ultrafast single-shot diffraction imaging of nanoscale dynamics," *Nature Phot.* **2**, 415–419 (2008).

[4] Wachulak, P. W., Marconi, M. C., Bartels, R. A., Menoni, C. S., and Rocca, J. J., "Soft X-ray laser holography with wavelength resolution," *Opt. Express* **15**, 10622 (2007).

[5] Filevich, J., Kanizay, K., Marconi, M. C., Chilla, J. L. A., and Rocca, J. J., "Dense plasma diagnostics with an amplitude-division soft-X-ray laser interferometer based on diffraction gratings," *Opt. Lett.* **25**, 356 (2000).

[6] Hinnen, P. C., Werners, S. E., Stolte, S., Hogervorst, W., and Ubachs, W., "XUV-laser spectroscopy of HD at 92Ű98 nm," *Phys. Rev. A* **52**, 4425 (1995).

[7] Lin, J., Weber, N., Maul, J., Hendel, S., Rott, K., Merkel, M., Schoenhense, G., and Kleineberg, U., "At-wavelength inspection of sub-40 nm defects in extreme ultraviolet lithography mask blank by photoemission electron microscopy," *Opt. Lett.* **32**, 1875 (2007).

[8] Cavalieri, A. L., Müller, N., Uphues, T., Yakovlev, V. S., Baltuska, A., Horvath, B., Schmidt, B., Blümel, L., Holzwarth, R., Hendel, S., Drescher, M., Kleineberg, U., Echenique, P. M., Kienberger, R., Krausz, F., and Heinzmann, U., "Attosecond spectroscopy in condensed matter," *Nature* **449**, 1029 (2007).

[9] Gohle, C., Udem, T., Herrmann, M., Rauschenberger, J., Holzwarth, R., Schuessler, H. A., Krausz, F., and Hänsch, T. W., "A frequency comb in the extreme ultraviolet," *Nature* **436**, 234–237 (2005).

[10] Jones, R., Moll, K. D., Thorpe, M. J., and Ye, J., "Phase-coherent frequency combs in the vacuum ultraviolet via high-harmonic generation inside a femtosecond enhancement cavity," *Phys. Rev. Lett.* **94**, 193201 (2005).

[11] Hartl, I., Schibli, T. R., Marcinkevicius, A., Yost, D. C., Hudson, D. D., Fermann, M. E., and Ye, J., "Cavity-enhanced similariton yb-fiber laser frequency comb: 3×10^{14} W/cm^2 peak intensity at 136MHz," *Opt. Lett.* **32**, 2870–2872 (2007).

[12] Ozawa, A., Rauschenberger, J., Gohle, C., Herrmann, M., Walker, D. R., Pervak, V., Fernandez, A., Graf, R., Apolonski, A., Holzwarth, R., Krausz, F., Hänsch, T., and Udem, T., "High harmonic frequency combs for high resolution spectroscopy," *Phys. Rev. Lett.* **100**, 253901 (2008).

[13] Yost, D. C., Schibli, T. R., and Ye, J., "Efficient output coupling of intracavity high harmonic generation," *Opt. Lett.* **33**, 1099–1101 (2008).

[14] Pupeza, I., Eidam, T., Rauschenberger, J., Bernhardt, B., Ozawa, A., Fill, E., Apolonski, A., Udem, T., Limpert, J., Alahmed, Z. A., Azzeer, A. M., Tünnermann, A., Hänsch, T. W., and Krausz, F., "Power scaling of a high repetition rate enhancement cavity," *Opt. Lett.* **12**, 2052–2054 (2010).

[15] Rempe, G., Thompson, R. J., Kimble, H. J., and Lalezari, R., "Measurement of ultralow losses in an optical interferometer," *Opt. Lett.* **17**, 363–365 (1992).

[16] Cingöz, A., Yost, D. C., Ye, J., Ruehl, A., Fermann, M., and Hartl, I., "Power scaling of high-repetition-rate HHG," *International Conference on Ultrafast Phenomena* (2010).

[17] Pupeza, I., Gu, X., Fill, E., Eidam, T., Limpert, J., Tünnermann, A., Krausz, F., and Udem, T., "Highly sensitive dispersion measurement of a high-power passive optical resonator using spatial-spectral interferometry," *Opt. Express* **18**, 26184–26195 (2010).

[18] Udem, T., Holzwarth, R., and Hänsch, T. W., "Optical frequency metrology," *Nature* **16**, 233–237 (2002).
[19] Eidam, T., Röser, F., Schmidt, O., Limpert, J., and Tünnermann, A., "57 W, 27 fs pulses from a fiber laser system using nonlinear compression," *Appl. Phys. B* **92**, 9 (2008).
[20] Hänsch, T. and Couillaud, B., "Laser frequency stabilization by polarization spectroscopy of a reflecting reference cavity," *Opt. Comm.* **35**, 441 (1980).
[21] Paschotta, R., "Beam quality deterioration of lasers caused by intracavity beam distortions," *Opt. Express* **14**, 6069–6074 (2006).
[22] Yang, Y.-Y., Süssmann, F., Zherebtsov, S., Pupeza, I., Kaster, J., Lehr, D., Kley, E.-B., Fill, E., Duan, X.-M., Zhao, Z.-S., Krausz, F., Stebbings, S., and Kling, M. F., "Optimization and characterization of a highly-efficient diffraction nanograting for MHz XUV pulses," *submitted to Opt. Express* (2010).
[23] Weitenberg, J., Russbüldt, P., Eidam, T., and Pupeza, I., "Quasi-imaging in a high-finesse femtosecond enhancement cavity," *in preparation* (2011).
[24] Eidam, T., Hanf, S., Seise, E., Andersen, T. V., Gabler, T., Wirth, C., Schreiber, T., Limpert, J., and Tünnermann, A., "Femtosecond fiber CPA system emitting 830W average output power," *Opt. Lett.* **35**, 94–96 (2010).
[25] Martin, F., Fernandez, J., Havermeier, T., Foucar, L., Weber, T., Kreidi, K., Schöffler, M., Schmidt, L., Jahnke, T., Jagutzki, O., Czasch, A., Benis, E. P., Osipov, T., Landers, A. L., Belkacem, A., Prior, M. H., Schmidt-Böcking, H., Cocke, C. L., and Dörner, R., "Single photon-induced symmetry breaking of H2 dissociation," *Science* **31**, 629–633 (2007).
[26] Fittinghoff, D. N., Bolton, P. R., Chang, B., and Kulander, K. C., "Observation of nonsequential double ionization of helium with optical tunneling," *Science* **69**, 2642–2645 (1992).
[27] Moshammer, R., Feuerstein, B., Lopez-Urrutia, J. C., Deipenwisch, J., Dorn, A., Fischer, D., Höhr, C., Neumayer, P., Schröter, C. D., Ullrich, J., Rottke, H., Trump, C., Wittmann, M., Korn, G., and Sandner, W., "Correlated two-electron dynamics in strong-field double ionization," *Phys. Rev. A* **65**, 035401 (2002).
[28] Ullrich, J., Moshammer, R., Dorn, A., Dörner, R., Schmidt, L. P. H., and Schmidt-Böcking, H., "Recoil-ion and electron momentum spectroscopy: reaction-microscopes," *Rep. Prog. Phys.* **66**, 1463 (2003).
[29] Stockman, M. I., Kling, M. F., Kleineberg, U., and Krausz, F., "Attosecond nanoplasmonic-field microscope," *Nature Phot.* **1**, 539 (2007).
[30] Mikkelsen, A., Schwenke, J., Fordell, T., Luo, G., Klünder, K., Hilner, E., Anttu, N., Zakharov, A. A., Lundgren, E., Mauritsson, J., Andersen, J. N., Xu, H. Q., and L'Huillier, A., "Photoemission electron microscopy using extreme ultraviolet attosecond pulse trains," *Rev. Sci. Instr.* **80**, 123703 (2009).
[31] Hartemann, F. V., Brown, W. J., Gibson, D. J., Anderson, S. G., Tremaine, A. M., Springer, P. T., Wootton, A. J., Hartouni, E. P., and Barty, C. P. J., "High-energy scaling of compton scattering light sources," *Phys. Rev. ST Accel. Beams* **8**, 100702 (2005).
[32] Sakaue, K., Washio, M., Araki, S., Fukuda, M., Higashi, Y., Honda, Y., Omori, T., Taniguchi, T., Terunum, N., Urakawa, J., and Sasao, N., "Observation of pulsed X-ray trains produced by laser-electron Compton scatterings," *Rev. Scientific. Instrum.* **80**, 123304 (2009).
[33] Krischek, R., Wieczorek, W., Ozawa, A., Kiesel, N., Michelberger, P., Udem, T., and Weinfurter, H., "Ultraviolet enhancement cavity for ultrafast nonlinear optics and high-rate multiphoton entanglement experiments," *Nature Phot.* **4**, 170 (2010).
[34] Motsch, M., Zeppenfeld, M., Pinkse, P. W. H., and Rempe, G., "Cavity-enhanced rayleigh scattering," *New J. of Physics* **12**, 063022 (2010).
[35] Gohle, C., Stein, B., Schliesser, A., Udem, T., and Hänsch, T. W., "Frequency comb vernier spectroscopy for broadband, high resolution, high sensitivity absorption and dispersion spectra," *Phys. Rev. Lett.* **99**, 263902 (2007).
[36] Herrmann, M., Haas, M., Jentschura, U. D., Kottmann, F., Leibfried, D., Saathoff, G., Gohle, C., Ozawa, A., Batteiger, V., Knünz, S., Kolachevsky, N., Schüssler, H. A., Hänsch, T. W., and Udem, T., "Feasibility of coherent xuv spectroscopy on the $1S-2S$ transition in singly ionized helium," *Phys. Rev. A* **79**, 052505 (2009).
[37] Zavatta, A., Parigi, V., and Bellini, M., "Towards quantum frequency combs: Boosting the generation of highly nonclassical light states by cavity-enhanced parametric down-conversion at high repetition rates," *Phys. Rev. A* **78**, 033809 (2008).